8-18-2021

Cortical Microstructural Changes Associated With Treated Aphasia Recovery

Allen J. Chang

Janina Wilmonskoetter

Julius Fridriksson
FRIDRIKS@mailbox.sc.edu

Emilie R. McKinnon

Lorelei P. Johnson

See next page for additional authors

Publication Info

Published in *Annals of Clinical and Translational Neurology*, Volume 8, Issue 9, 2021, pages 1884-1894.

ANNALS of Clinical and Translational Neurology
Open Access
AMERICAN NEUROLOGICAL ASSOCIATION

RESEARCH ARTICLE

Cortical microstructural changes associated with treated aphasia recovery

Allen J. Chang[1,*], Janina Wilmskoetter[2,3,*], Julius Fridriksson[4], Emilie T. McKinnon[2], Lorelei P. Johnson[4], Alexandra Basilakos[4], Jens H. Jensen[5], Chris Rorden[6] & Leonardo Bonilha[2]

[1]College of Graduate Studies, Neuroscience Institute, Medical University of South Carolina, Charleston, South Carolina
[2]Department of Neurology, College of Medicine, Medical University of South Carolina, Charleston, South Carolina
[3]Department of Rehabilitation Sciences, College of Health Professions, Medical University of South Carolina, Charleston, South Carolina
[4]Department of Communication Sciences and Disorders, University of South Carolina, Columbia, South Carolina
[5]Department of Neuroscience, College of Medicine, Medical University of South Carolina, Charleston, South Carolina
[6]Department of Psychology, University of South Carolina, Columbia, South Carolina

Correspondence
Leonardo Bonilha, 96 Jonathan Lucas St, 3rd floor CSB, Department of Neurology, Medical University of South Carolina, Charleston 29425, SC. Tel: 843 792 5044; E-mail: bonilha@musc.edu

Funding Information
This study was supported by research grants from the National Institutes of Health/ National Institute on Deafness and Other Communication Disorders (NIDCD): DC014021 (PI: Bonilha), DC011739 (PI: Fridriksson), DC014664 (PI: Fridriksson), T32 DC014435 (Trainee: Basilakos, McKinnon) and from the American Heart Association: SFDRN26030003 (PI: Bonilha).

Received: 13 July 2021; Revised: 3 August 2021; Accepted: 3 August 2021

Annals of Clinical and Translational Neurology **2021; 8(9): 1884–1894**

doi: 10.1002/acn3.51445

*These authors contributed equally to the work.

Abstract

Objectives: To investigate the hypothesis that language recovery in post-stroke aphasia is associated with structural brain changes. **Methods**: We evaluated whether treatment-induced improvement in naming is associated with reorganization of tissue microstructure within residual cortical regions. To this end, we performed a retrospective longitudinal treatment study using comprehensive language-linguistic assessments and diffusion MRI sequences optimized for the assessment of complex microstructure (diffusional kurtosis imaging) to evaluate the relationship between language treatment response and cortical changes in 26 individuals with chronic stroke-induced aphasia. We employed elastic net statistical models controlling for baseline factors including age, sex, and time since the stroke, as well as lesion volume. **Results**: We observed that improved naming accuracy (Philadelphia Naming Test) was statistically associated with increased post-treatment microstructural integrity in the left posterior superior temporal gyrus. Moreover, increase in microstructural integrity in the left middle temporal gyrus and left inferior temporal gyrus was specifically associated with a decrease in semantic paraphasias. This longitudinal relationship between brain tissue integrity and language improvement was not observed in other non-language related brain regions. **Interpretation**: Our findings provide evidence that structural brain changes in the preserved left hemisphere regions are associated with treatment-induced language recovery in aphasia and are part of the mechanisms supporting language and brain injury recovery.

Introduction

Aphasia is the inability to process language and is a common functional deficit after a stroke.[1,2] Aphasia is typically associated with profound and negative consequences to social interactions, autonomy, and quality of life.[3] Approximately 40% of stroke survivors do not recover acutely, and go on to experience disabling, chronic language problems.[4] For individuals with chronic aphasia, language recovery can be achieved through speech and language therapy, but response to therapy is highly variable and the mechanisms underlying language recovery are not well understood.

A commonly hypothesized mechanism underlying recovery is brain plasticity, whereby gray matter structures that are partly damaged by the stroke may restore their functions or re-train to perform new functions.[5] Possible structural correlates of functional plasticity on the level of neuron populations are changes in grey matter thickness or density. While this is a promising and reasonable

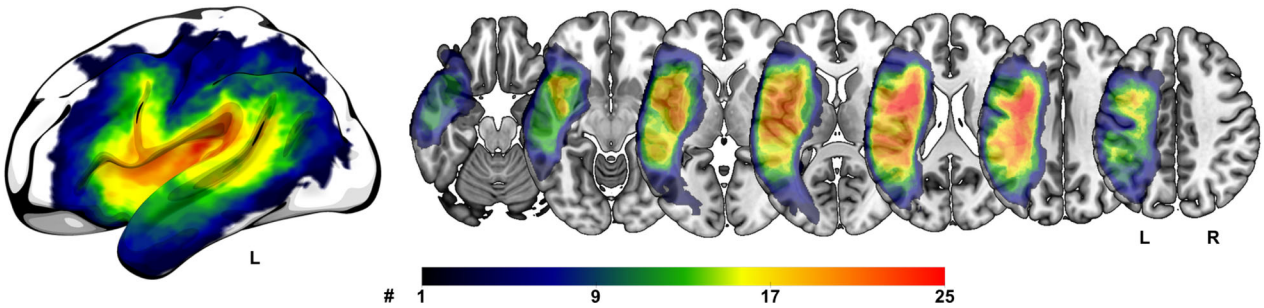

Figure 1. Lesion overlap map for all 26 included participants. Color bar indicates the number of participants with a lesion in that brain region. The warmer the color the more participants had a lesion in that region. L = left hemisphere, R = right hemisphere.

assumption, there is a lack of empirical demonstration concerning whether damaged structures do indeed recover in association with functional recovery. This lack of evidence impedes the development of further therapeutic and mechanistic advancements in aphasia recovery and stroke rehabilitation in general.

A likely explanation for the absence of evidence concerning in-vivo structural plasticity in humans is the difficulty in measuring subtle and complex microscopic changes thus far. However, novel and innovative forms of diffusion magnetic resonance imaging (dMRI) may now provide an adequate approach to assess subtle and complex brain microstructure, including longitudinal and clinically meaningful changes.[6] In particular, a novel dMRI approach to quantify brain tissue known as, diffusional kurtosis imaging (DKI),[7,8] may be especially useful in this context. DKI assesses non-Gaussian water diffusion properties, which are known to occur in the brain and provides more sensitive quantification of stroke related cellular and extracellular pathology.[9] In a pilot study, our group demonstrated microstructural re-strengthening in the inferior longitudinal fasciculus associated with aphasia treatment and a reduction in semantic naming errors.[10]

In this longitudinal treatment study, we tested the hypothesis that treatment-induced improvement in one form of speech production (naming) in the chronic stage of aphasia recovery would be associated with increased post-treatment microstructural integrity in gray matter regions related to language processing. We assessed retrospective data from individuals with chronic aphasia undergoing a Phase II clinical trial with a well-controlled treatment regimen as well as comprehensive language-linguistic and MRI assessment pre- and post-treatment. We used elastic net statistical models controlling for various baseline factors including age, sex, and time since the stroke along with lesion volume to assess if naming improvement was statistically associated with microstructural change, thus providing novel evidence in the mechanisms supporting recovery.

Table 1. Table summary of post-stroke aphasia participants.

Summary	Value
Participants, *N*	26 (8 female)
tDCS condition during language treatment, *N*	12-A-tDCS 14-S-tDCS
Highest year of school completed, mean ± SD	14 ± 2.4
Age in years, mean ± SD	57 ± 12
Time since stroke in months, mean ± SD	36 ± 31.2
WAB-AQ, mean ± SD	54 ± 20.3
Lesion size (mL), mean ± SD	163.54 ± 113.13

A-tDCS = anodal transcranial direct current stimulation; S-tDCS = sham transcranial direct current stimulation; WAB-AQ, aphasia quotient of the Western Aphasia Battery (revised).

Materials and Methods

Participants

Data analyzed in this study was obtained from a subset of participants who completed a Phase II clinical trial to evaluate the futility of transcranial direct current stimulation (tDCS) in aphasia treatment.[11] All participants had a history of single-event left-hemisphere ischemic stroke that resulted in aphasia. The subset of participants whose data were analyzed here include 33 individuals (10 Females; mean age of 58 years, standard deviation of 12 years) of the 74 participants of the original clinical trial. We chose this subset of participants based on the criteria that they underwent pre- as well as post-treatment MRI scans allowing longitudinal MRI-based analyses. Figure 1 presents a lesion overlap map for all participants. All participants were at least six months post-stroke, right-handed, native English speaking, and without a history of any other neurological disease affecting the brain (Table 1). All participants were recruited at the Medical University of South Carolina where the Institutional Review Board approved the study.

Upon study entry, participants were assessed for aphasia using the Western Aphasia Battery Revised (WAB-R).[12] Participants were classified as having aphasia if their quotient score fell below 93.8, in accordance with the assessment's conventions.

Computer-based aphasia training and t-DCS treatment

The behavioral treatment involved a computerized receptive naming test, where participants were shown a picture of an object, while viewing an audiovisual model of a speaker who either correctly or incorrectly named that object. Participants had to decide (yes/no response) if the picture matched the word the speaker produced. Incorrect matches were either semantically related, phonologically related, or unrelated foils. Trial by trial, participants could respond to correct matches with the press of a green button and to incorrect ones with a red button. Immediate incorrect or correct feedback followed each response alongside a display of the participant's accuracy. One hundred and sixty words (different from the PNT) were dedicated for this task.

While participants were undergoing the computerized treatment, they were randomized to receive either sham tDCS (S-tDCS) or active t-DCS (A-tDCS). Both treatment groups (S-tDCS and A-tDCS) received 3 weeks of the computer-based aphasia treatment with a total of 15 sessions within 21 days, each lasting 45-min.

Outcome measure: naming

In order to obtain quantifiable measures of functional change, participants were tested with the Philadelphia Naming Test (PNT).[13] The PNT is a naming task that includes the presentation of 175 drawings of mid to high frequency nouns to assess confrontation naming abilities. No PNT items were included in the computerized treatment program; thus, improvement on the PNT represents generalization from trained to untrained items. Naming accuracy was determined based on the PNT scoring guidelines with the exception to error types (semantic errors, phonological errors). Rather than scoring based on the first complete response, we scored errors based on the last attempt. We administrated the PNT twice at baseline and twice at 1-week post, to increase the reliability of participants' naming performance. We calculated the final scores for each time point by averaging the repeats.

Naming errors made on the PNT, and analyzed in this study, are as follows:

1 *Correct naming score* – number of correct naming attempts (naming accuracy).
2 *Semantic error score* – number of sematic paraphasias defined as when a semantically related but different word is substituted for the intended word (ex: "leg" instead of "hand").
3 *Phonological error score* – number of phonological paraphasias defined as a replacement of a word with a similar sounding nonword in which at least 50% of the segments and/or number of syllables of the intended word is preserved (ex: "mook" instead of "book").

Neuroimaging

Participants underwent dMRI pre-treatment and 1 week after the completion of therapy. To measure microstructural changes in gray matter, we calculated kurtosis tensors (Figure 2). Overall, increase of mean kurtosis is a biophysical measure of tissue change and likely reflects an increase of intact structures like cell membranes and organelles which restrict water diffusion in the gray matter.[9]

All participants were scanned at the Medical University of South Carolina using a Siemens 3 T TIM Trio MRI scanner (Siemens Healthcare, Erlangen, Germany) with a 12-channel head coil. A total of 131 volumes were collected in three series, each with three degrees of diffusion weighting (b-value=0, 1000, 2000 s/mm^2): 30 diffusion-encoding directions were acquired twice, for both $b = 1000$ and 2000 s/mm^2, and eleven without diffusion weighting ($b = 0$). Some additional parameters were pixel bandwidth = 1355 Hz/px, $2.7 \times 2.7 \times 2.7$ mm^3 isotropic voxels, TR = 6100 msec, TE = 101 msec. To minimize the contributions of eddy currents, we acquired all diffusion-weighted images (DWI) using a twice-refocused gradient scheme and without partial Fourier encoding. We utilized a 3D-TSE SPACE protocol (160 sagittal slices, field of view (FOV) = 256×256 mm^2, TE = 212 msec, TR = 3200 msec, echo trains per slice = 2, echo train duration = 432 msec, turbo factor = 129) to collect high resolution 1 mm^3 isotropic T2-weighted images. For anatomical reference, we gathered T1-weighted images using 1 mm MPRAGE sequence: TI = 925 msec, TR = 2250 msec, TE = 4.15 msec, FOV=256-$\times$ 256 mm^2, 9° flip angle.

Diffusion and kurtosis tensors were estimated using publicly available processing software: Nii_preprocess (https://github.com/neurolabusc/nii_preprocess/). Raw dMRI images were denoised,[14] corrected for Gibbs ringing,[15] coregistered (FMRIB Software Library v5.0), and smoothed before estimating the tensors using MRtrix3 dwi2tensor. Imaging processing and analysis were performed in MATLAB R2019b using in-house developed scripts and SPM12 (version 7487) (Functional Imaging Laboratory, Wellcome Trust Centre for Neuroimaging Institute of Neurology, University College London; http://www.fil.ion.ucl.ac.uk/spm/software/spm12/). Readers are referred to Fridriksson et al., 2018 for details pertaining to behavioral and neuroimaging methods.

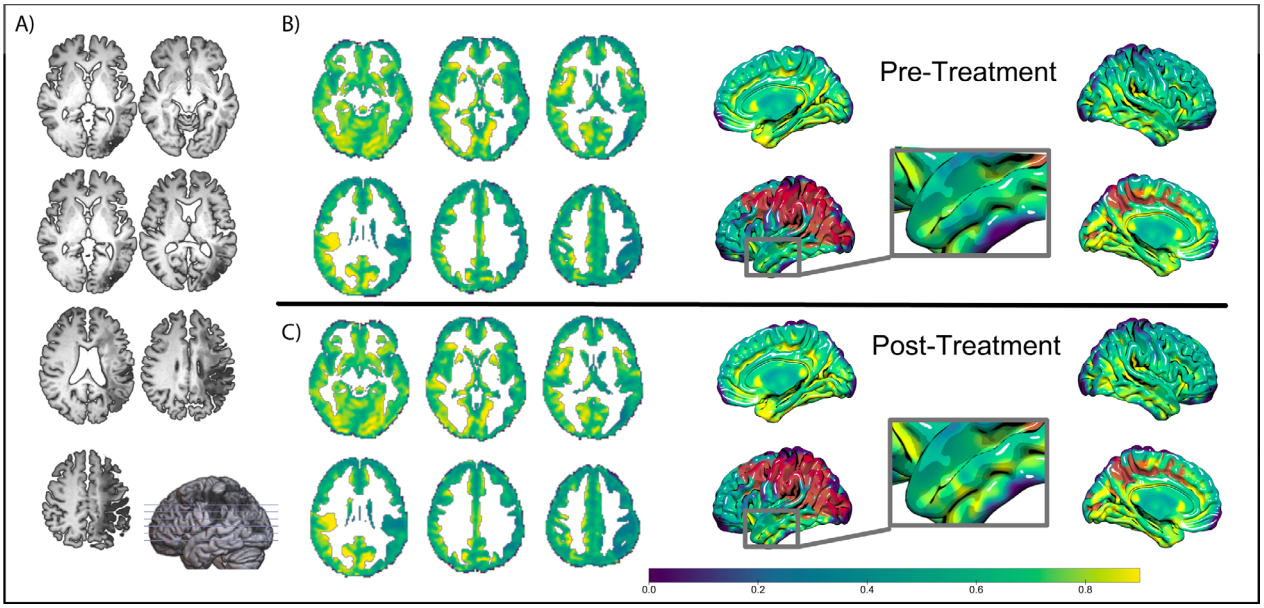

Figure 2. Representative example of magnetic resonance images obtained from one subject. Blue-green-yellow color bar represents mean kurtosis measurements. Red color indicates lesion. (A) T1-weighted slices with 3D model. (B) Pre-treatment mean kurtosis slices with 3D model. (C) Post-treatment mean kurtosis slices with 3D model.

Regions of interest

Structural analysis was restricted to language specific regions of interests (ROIs) in the left hemisphere cortical gray matter and its homologous right hemisphere structures. Although the specific brain regions associated with the dorsal stream and ventral stream are debated, we defined these two streams based on our previous study[16] and on Hickok & Poeppel 2007[17] using the John Hopkins University (JHU) atlas (15 left hemisphere ROIs). In the left hemisphere dorsal stream, structures included the inferior frontal gyrus pars opercularis, inferior frontal gyrus pars triangularis, postcentral gyrus, precentral gyrus, supramarginal gyrus, anterior insula, and posterior insula. The ventral stream in the left hemisphere included the inferior frontal gyrus pars orbitalis, angular gyrus, superior temporal gyrus, pole of superior temporal gyrus, middle temporal gyrus, inferior temporal gyrus, posterior superior temporal gyrus, and posterior middle temporal gyrus. In addition to the 15 left hemisphere regions, we included the 15 homologous structures in the right hemisphere to discern potential contributions of the right hemisphere for treated aphasia recovery. Thus, in total we included 30 brain regions in our analyses (visualized in Fig. S1). Although we only defined the language streams in the left hemisphere, it is assumed that the ventral stream is bilateral while the dorsal stream is primarily left lateralized.

Statistical analysis

We used elastic net regularization to identify a set of predictors balancing the highest possible predictive value with parsimonious variable selection. Elastic net regularization is a regularized regression model that is particularly useful in cases with a multitude of variables, and that potentially show multicollinearity (as it commonly occurs in gene analysis and machine learning[18,19]). In short, it combines the penalties of lasso and ridge regularization methods. Here we applied ridge and lasso regularizations in 0.1 and 0.02 increments, respectively, from 0 (min) to 1 (max). Ten-fold cross-validation was used to identify the best parsimonious model (convergence criterion: 0.00001 with max. 100 iterations) from a set of candidate independent variables listed below.

Three dependent variables were evaluated by separate elastic net models:

1 *Change in correct naming* – Change in correct naming responses from baseline to 1 week after treatment. Correct responses were calculated as the change of correct responses from baseline to 1 week after treatment over the room to improve at baseline

$$\left(\frac{\text{ofcorrectresponsesat1week} - \text{ofcorrectresponsesatbaseline}}{175 - \text{numberofcorrectresponsesatbaseline}} \times 100.\right)$$

2 *Change in semantic errors* – Change in the semantic error score from baseline to 1 week after treatment.

Semantic errors were calculated as the percentage of semantic errors over the number of naming attempts

$$\left(\frac{\text{ofsemanticerrorsat1week}}{\text{ofattemptsat1week}} - \frac{\text{ofsemanticerrorsatbaseline}}{\text{ofattemptsatbaseline}}\right) \times 100.$$

3 *Change in phonological errors* – Change in the phonological error score from baseline to 1 week after treatment. Phonological errors were calculated as the percentage of phonological errors over the number of naming attempts

$$\left(\frac{\text{ofphonologicalerrorsat1week}}{\text{ofattemptsat1week}} - \frac{\text{ofphonologicalerrorsatbaseline}}{\text{ofattemptsatbaseline}}\right) \times 100.$$

Candidate independent variables included in each of the three elastic net models (unless otherwise noted):

1 *Baseline Mean Kurtosis (each of the 30 regions)* – mean kurtosis for each region of interest before treatment.
2 *Change in Mean Kurtosis (each of the 30 regions)* – change in mean kurtosis (from 1 week after the treatment compared to baseline) for each region of interest.
3 *Treatment* – whether participants received A-tDCS (value of 1) or S-tDCS (value of 0).
4 *Sex* – reported sex of participants (Male or Female).
5 *Lesion volume* – lesion volume in ml obtained by manually drawn lesion maps.
6 *Education* – years of completed education – used as a continuous variable in the model (for reference, 12 years indicate a high school diploma, 16 years indicate an undergraduate degree, 17 or more years indicate a graduate degree).
7 *Age* – reported age of each participant in years.
8 *Time since stroke* – time since initial stroke event in months.
9 *WAB-AQ* – aphasia quotient of the Western Aphasia Battery (revised).
10 *Room to improve (limited to the model for change in correct naming)* – difference between baseline correct responses and highest possible correct naming score (175 - number of correct responses at baseline).
11 Percent attempts baseline *(limited to model for change in semantic errors and change in phonological errors)* – percent of naming attempts for all 175 items (number of attempts at baseline/175).

Elastic net models were generated using IBM Statistical Package for the Social Sciences (SPSS) program for Windows (version 25, released 2017, IBM Corp., Armonk, N.Y., USA). Pearson's correlation coefficient test was run on GraphPad Prism 6 for windows (Version 6.01, released 2012, GraphPad Software Inc.). Participants that did not have complete data sets were omitted from analysis.

Results

The term "predictors" from here onwards will be used for variables that were obtained before treatment (baseline) and were associated to be predictive of pre- to post-treatment naming changes. "Associations" will be used for variables that were measured pre- and post-treatment whose changes were hypothesized to be associated with changes in pre- to post-treatment naming.

Functional change

Participants displayed high variability in response to treatment as summarized in Figure 3. For all 175 items in the PNT, participants produced on average 49.5 (28.3%) correct responses before and 55.9 (31.9%) correct responses after treatment. Out of the 26 participants, 17 made more correct naming responses from before to after treatment, seven participants made fewer correct responses, and two showed no change in the number of correct responses.

Semantic errors were observed with an average of 20 responses (11.4%) before and 16.6 (9.5%) responses after treatment. Twenty participants made fewer errors after treatment, six participants made more errors after treatment, and zero participants showed no change in the number of semantic errors from baseline to 1 week after treatment. Phonological errors occurred less often than semantic errors. On average 10.6 responses (6%) were phonological errors before and 8.8 responses (5%) after treatment. Out of the 26 participants, 12 made fewer, 11 made more, and three made an equal number of phonological errors after treatment.

Additionally, we ran Pearson's correlation analysis on the three dependent variables to examine if there was any relationship between them. All tests came out statistically non-significant (p value >0.05). The change in correct naming did not correlate with the change in semantic errors (correlation coefficient = 0.06, p value = 0.75), the change in correct naming did not correlate with the change in phonological errors (correlation coefficient = -0.27, p value = 0.17), and the change in semantic errors did not correlate with the change in phonological errors (correlation coefficient = -0.28, p value = 0.14).

Predictors and associations

To investigate potential predictors/associations of treatment outcome, we created three separate elastic net models for each dependent variable: one for change in correct

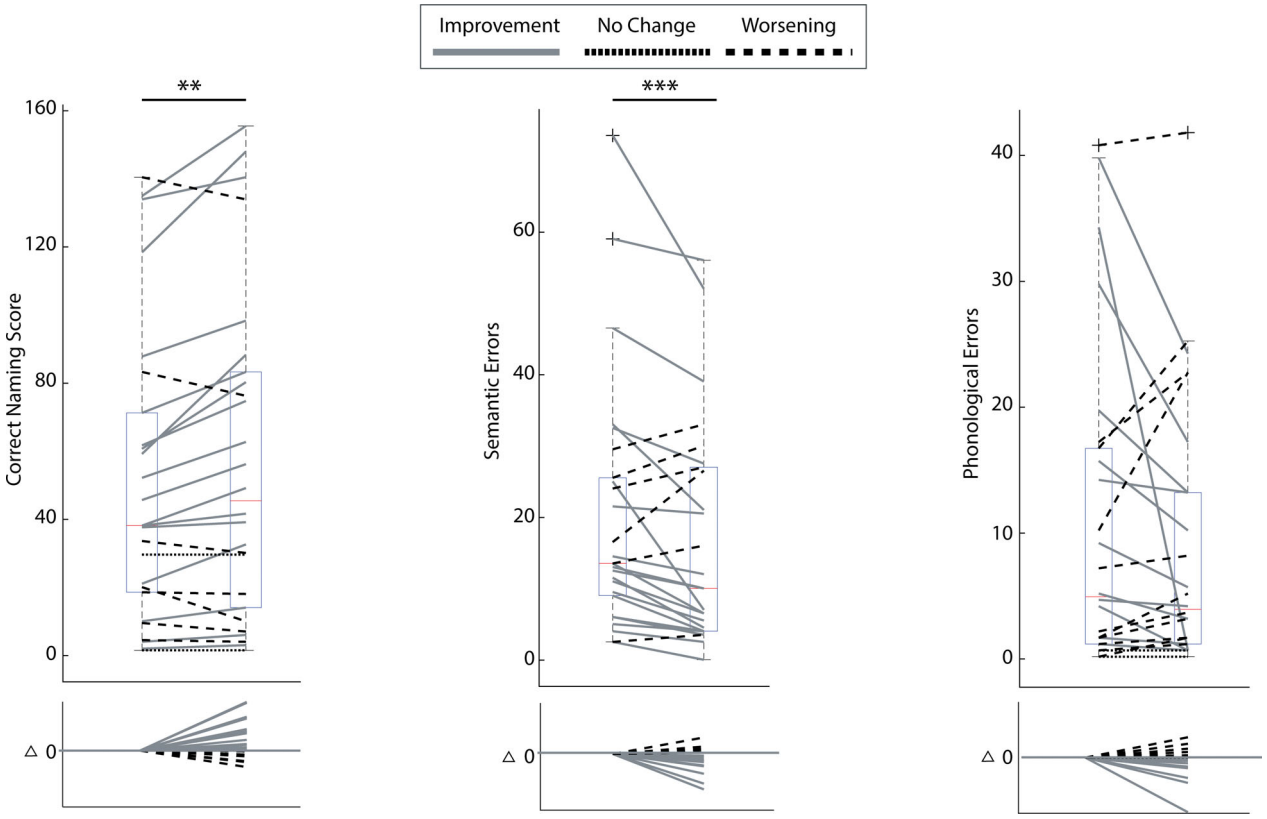

Figure 3. Box charts summarize participant performance on the Philadelphia Naming Test at baseline and 1-week post-treatment. The central mark indicates the median while the 25th and 75th percentiles are indicated by the bottom and top edges of the box, respectively. The whiskers indicate the most extreme non-outlier data points, and the "x" symbols indicate the outliers. (A) Correct naming score – number of correct attempts; (B) semantic error score – number of semantic paraphasias; (C) phonological error score – number of phonological paraphasias. Solid lines indicate improvement, doted lines indicate no change, and dashed lines indicate worsening from baseline to 1-week post-treatment.

naming, one for change in semantic errors, and one for change in phonological errors. This model eliminated nonsignificant independent variables, leaving the most influential predictors/associations in the final models.

The elastic net model computed for the dependent variable change in correct naming (Table 2) had an R-square value of 0.616 with a sample size of 26. The selected model included seven independent variables: six predictors and one association. Structural predictors included in the final model were (1) baseline mean kurtosis in the left postcentral gyrus (beta = −0.069), (2) left supramarginal gyrus (beta = −0.173), (3) and left angular gyrus (beta = −0.185). Associations included in the model were (4) change in mean kurtosis in the left posterior superior temporal gyrus (beta = 0.003). Non-structural predictors included in the final model were (5) whether participants received concurrent A-tDCS (beta coefficient of 0.74), (6) years of education (beta = 0.142), and (7) anomia severity (measured by correct naming *room to improve at baseline*; beta = −0.179). A positive beta-coefficient refers to a positive relationship between the independent and dependent variable and vice versa. For example, in the model for change in correct naming, the variable "education" had a beta value of 0.142. This means that for every 1.0 unit increase in the variable "education" (i.e., 1 year of education), there was a predicted increase of 0.142 in change in correct naming. Brain maps of the beta-coefficients of the elastic net model with the dependent variable change in correct naming are displayed in Figure 4.

The computed elastic net model for the dependent variable change in semantic errors (Table 2) had an *R*-square value of 0.425 with a sample size of 25 (1 sample was discarded due to incomplete data). The selected model included two associations: (1) change in mean kurtosis in the left middle temporal gyrus (beta = −0.031) and (2) change in mean kurtosis in the left inferior temporal gyrus (beta = −0.108). Brain maps of the beta-coefficients of the elastic net model with the dependent variable change in semantic errors are displayed in Figure 4.

The computed elastic net model for the dependent variable change in phonological errors (Table 2) had an

Table 2. Table summary of elastic net regularization models created for each dependent variable.

Dependent variable	Change in correct naming	Change in semantic errors	Change in phonological errors
R square	0.616	0.425	0.158
Number of participants	26	25	24
Predictors	Mean kurtosis at baseline • Postcentral gyrus left (–0.069) • Supramarginal gyrus left (–0.173) • Angular gyrus left (-0.185) Non-structural • tDCS type (0.74) • Education (0.142) • Room to improve in correct naming at baseline (–0.179)		Mean kurtosis at baseline • Posterior Insula left (-0.008)
Associations	Change in mean kurtosis • Posterior superior temporal gyrus left (0.003)	Change in mean kurtosis • Middle temporal gyrus left (–0.031) • Inferior temporal gyrus left (–0.108)	

The dependent variable change in correct naming was calculated as ((correct at 1 week) – (correct at baseline))/(175 – (correct at baseline)) *100. The dependent variable change in semantic errors was calculated as ((percent semantic errors at 1 week) – (percent semantic errors at baseline)). The dependent variable change in phonological errors was calculated as ((percent phonological errors at 1 week) – (percent phonological errors at baseline)). The number in parenthesis indicates the beta coefficient for that variable in the model.

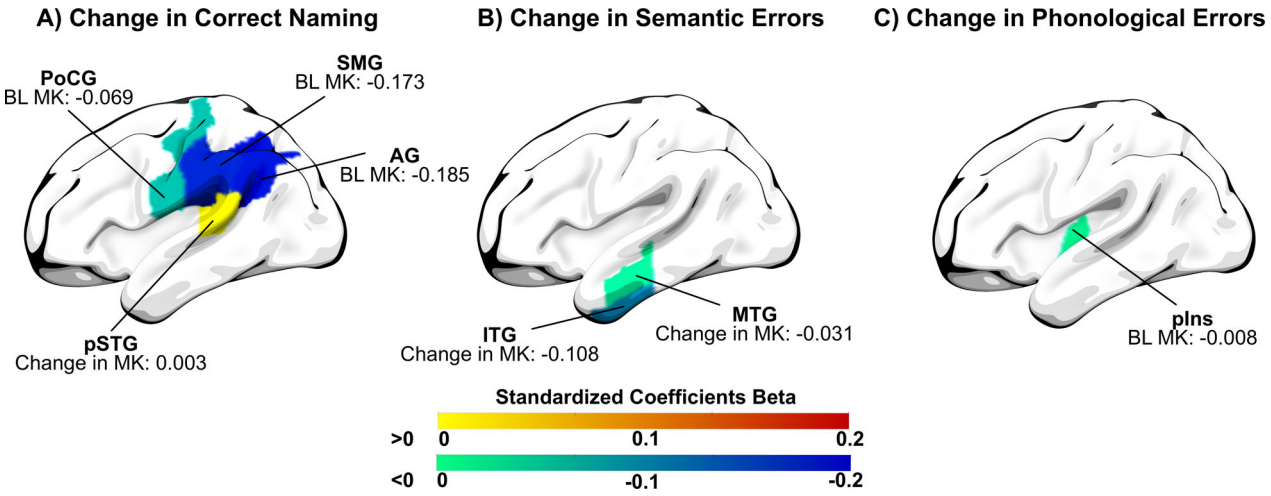

Figure 4. Structural predictors and associations included in the final elastic net models for the dependent variables (A) change in correct naming, (B) change in semantic errors, and (C) Change in Phonological Errors. Numbers are the standardized coefficients beta for each region. Warm colors represent positive coefficients beta, cold colors represent negative coefficients beta. MK = mean kurtosis; BL = baseline; AG = angular gyrus; PoCG = postcentral gyrus; pSTG = posterior superior temporal gyrus; SMG = supramarginal gyrus; IFG = inferior frontal gyrus, MTG = middle temporal gyrus; pIns = posterior Insula.

R-square value of 0.158 with a sample size of 24 (2 samples were discarded due to incomplete data). The selected model included one predictor: baseline mean kurtosis in the left posterior insula (−0.008).

In post-hoc analyses we assessed the relationship between lesion volume and mean kurtosis for each region selected in the elastic net models as significant predictor or association with treatment outcome. We conducted univariate regression modeling and visual inspection of scatterplots for responders (better naming performance after treatment) and non-responders (worse naming performance after treatment). Figures S2, S6, and S7 show that there was no significant relationship between regional lesion volume and change in mean kurtosis for the

posterior superior temporal gyrus, middle temporal gyrus and inferior temporal gyrus. In contrast, regional lesion volume was significantly related to baseline mean kurtosis for the postcentral gyrus, supramarginal gyrus, angular gyrus, and posterior insula as shown in Figures S3, S4, and S8.

Discussion

Our main objective was to assess the relationship between improvement in naming and microstructural grey matter, cortical integrity in individuals with chronic aphasia. We build on our previous study by McKinnon et al., where we reported structural changes in white matter tracts (i.e., left inferior longitudinal fasciculus) associated with improvement of semantic paraphasias.[10] The study presented here is an extension and expansion of the study by McKinnon et al., analyzing more subjects (from 8 to 26) and expanding analysis to gray matter structures. Our use of DKI allowed us to examine longitudinal structural changes and predictors associated with naming improvement.

Change in mean kurtosis

We found a significant association between the increase of mean kurtosis in language-related cortical regions and improved naming performance from before to after treatment. While an increase in mean kurtosis does not always reflect an improvement in brain microstructure,[9] previous evidence suggests that, at least in gray matter of individuals with a chronic stroke, an increase in kurtosis typically relates to an increase of intact structures in brain tissue.[9,20] Thus, change in grey matter kurtosis from before to after the language training could potentially reflect one or a combination of two types of mechanisms: change in gray matter neurons (e.g., axonal sprouting, dendritic branching synaptogenesis, or neurogenesis) or change in gray matter neuronal support cells (e.g., astrocyte/microglial change in number or morphology).[21] The underlying neurophysiological mechanisms of kurtosis change were beyond the scope of this study. Nevertheless, a change in mean kurtosis occurred in grey matter independently of how much or if the region was at all damaged. Thus, our results support both phenomena indicating that gray matter changes occurred in areas compromised by the stroke as well as in areas spared by the stroke.

In terms of correct naming, we observed that a treatment-related increase in mean kurtosis in the left posterior superior temporal gyrus was associated with an increase in correct naming responses after treatment. This observation is in synchrony with the vast literature on the importance of the superior temporal gyrus to language.[22–25] The left posterior superior temporal gyrus, often referenced as part of Wernicke's area, may constitute a "hub" within the language network, meaning that this region is particularly well linked to other language-related regions, and is involved in naming and multiple other language tasks.[22] It may coordinate activity between the ventral and dorsal language streams[17,26] and lesions to the posterior superior temporal gyrus have been related to profound impairment in language processing.[22]

In terms of semantic errors, we observed a relationship between decreased numbers of semantic errors and increased microstructural integrity of the left middle temporal gyrus and left inferior temporal gyrus. These results are in line with previous research suggesting that the middle temporal gyrus and the left inferior temporal gyrus are associated with semantic control, and belong to the ventral stream of language processing.[16,27,28] Our longitudinal findings provide additional evidence that not only do these regions support semantic processing, but they are also important for treated reductions in semantic paraphasias.

The change in mean kurtosis in the posterior superior temporal gyrus, middle temporal gyrus, and inferior temporal gyrus occurred independently of how much these regions were directly affected by the stroke lesion (see supplementary Figures). This was the case for individuals who improved after treatment as well as for individuals who did not improve after treatment. The lack of a relationship between the predictive power of the change in gray matter integrity in these regions and their lesion volume suggests that crucial microstructural treatment-induced brain changes are not necessarily dependent on how much or little a brain region was damaged by the stroke. Because all three regions have in common that they are part of the language network, the functional role of regions in language processing (before and/or after the stroke) might be more important why microstructural changes support treated recovery as compared to the lesion affecting a region. Thus, our results suggest that meaningful microstructural changes can occur in regions independently of their underlying structural damage. Nevertheless, because values for lesion volume and mean kurtosis were averages for each brain region in our study, future studies are warranted to localize the crucial microstructural changes more precisely regarding the underlying tissue properties whether changes occur in lesioned or/and spared tissue.

Importantly, in our study we observed associative relationships, but we cannot infer a direct causal relationship between changes in brain microstructure and correct naming. Our findings encourage future studies to assess how aphasia treatment can impact the microstructural integrity of targeted regions and how these changes relate to language improvements.

Mean kurtosis at baseline

We observed that baseline microstructural integrity in specific regions was associated with better naming performance after treatment. This finding suggests that, not only does an individual's treatment response seem to depend on the tendency of specific regions to undergo plastic changes throughout treatment, but also on the baseline integrity of specific regions. Similarly, the degree of baseline functional impairment (or the room to improve) is a well-known crucial predictor for treatment outcome of individuals with post-stroke aphasia.[29,30] Thus, our study adds to the current evidence that both baseline functional impairment and baseline structural integrity are markers for treated naming recovery.

In our study, better baseline microstructural integrity of the left posterior insula predicted fewer phonological errors (better improvement) after treatment. While baseline microstructural integrity of the insula was the only selected predictor, the model had a low overall performance (R-square = 0.158) ultimately providing relatively limited predictive value. Reasons for the unsatisfying model performance may reflect fewer phonological errors across individuals at baseline and the even smaller change in phonological errors after treatment.

While we found a positive relationship between baseline structural integrity and improvement in phonological errors, we found a negative relationship between baseline structural integrity and improvement in correct naming after treatment. In several regions (the left postcentral, supramarginal, and angular gyri) lower baseline microstructural integrity predicted better improvement in naming accuracy after treatment. It remains speculative why worse and not better baseline microstructure predicted better treatment responses. Not surprising, we found a strong relationship between baseline mean kurtosis and regional lesion volume (see supplementary Figures). The higher the lesion load to a region the lower was the region's microstructural integrity. Thus, a possible explanation why worse microstructure predicted improvement is the mutual exclusivity of lesions to certain brain regions. Mutual exclusivity is defined by the phenomenon where damage caused by a stroke to one brain region typically spares another region. This is largely due to the architecture of the brain. For example, aphasia is most caused by strokes in the middle cerebral artery (MCA). The MCA divides into two major branches, the superior and inferior branch. Across individuals, it is generally recognized that strokes localized to the superior branch cause lesions in some regions while sparing other regions, and strokes in the inferior branch tend to show the opposite pattern regarding which regions are lesioned or spared. Thus, individuals might benefit from treatment depending on which regions were spared by the lesion and not which regions were lesioned. Mutual exclusivity could be a mechanism that explains why lower baseline microstructural integrity predicts better naming improvement, but further research is necessary for more definitive conclusions in this regard.

Right hemisphere homologous structures

We included left hemisphere ROIs and their right hemisphere homologous structures as candidate factors in our analyses. Microstructural integrity (baseline and/or change) of the right hemisphere homologous structures did not provide any additional predictive value for the elastic net models fitted for the three dependent variables. While previous research suggests the involvement of the right hemisphere in aphasia recovery,[31,32] our data indicate that the predictive value of microstructural integrity for treatment induced improvement is solely restricted to language related regions in the left hemisphere. Our findings do not necessarily negate an involvement of the right hemisphere in aphasia recovery but suggest structural integrity and plasticity in the left hemisphere is more salient. Indeed, other group have suggested involvement of the right hemisphere in post-stroke aphasia recovery.[33–35]

Acknowledgments

This study was supported by research grants from the National Institutes of Health/National Institute on Deafness and Other Communication Disorders (NIDCD): DC014021 (PI: Bonilha), DC011739 (PI: Fridriksson), DC014664 (PI: Fridriksson), T32 DC014435 (Trainee: Basilakos, McKinnon) and from the American Heart Association: SFDRN26030003 (PI: Bonilha).

Author Contributions

L.B. and J.F. designed the research; A.C. and J.W. performed the analyses; E.T.M., J.J. and C.R. processed the MRI data; A.B. and L.P.J. collected the behavioral and MRI data; A.C. and J.W. wrote the paper; L.B., J.F., A.B., L.P.J., E.T.M., J.J., and C.R. critically revised the paper.

Conflicts of Interest

Nothing to report.

References

1. Engelter ST, Gostynski M, Papa S, et al. Epidemiology of aphasia attributable to first ischemic stroke: incidence, severity, fluency, etiology, and thrombolysis. Stroke. 2006;37(6):1379–1384.

2. Mitchell C, Gittins M, Tyson S, et al. Prevalence of aphasia and dysarthria among inpatient stroke survivors: describing the population, therapy provision and outcomes on discharge. Aphasiology. 2020;35(7):950–960.
3. Koleck M, Gana K, Lucot C, Darrigrand B, Mazaux JM, Glize B. Quality of life in aphasic patients 1 year after a first stroke. Qual Life Res. 2017;26(1):45–54.
4. Wade DT, Hewer RL, David RM, Enderby PM. Aphasia after stroke: natural history and associated deficits. J Neurol Neurosurg Psychiatry. 1986;49(1):11–16.
5. Warraich Z, Kleim JA. Neural plasticity: the biological substrate for neurorehabilitation. PM&R. 2010;2(12):S208–S219. http://10.0.3.248/j.pmrj.2010.10.016
6. Crosson B, Rodriguez AD, Copland D, et al. Neuroplasticity and aphasia treatments: new approaches for an old problem. J Neurol Neurosurg Psychiatry. 2019;90(10):1147–1155.
7. Jensen JH, Helpern JA. MRI quantification of non-Gaussian water diffusion by kurtosis analysis. NMR Biomed. 2010;23(7):698–710.
8. Jensen JH, Helpern JA, Ramani A, Lu H, Kaczynski K. Diffusional kurtosis imaging: the quantification of non-gaussian water diffusion by means of magnetic resonance imaging. Magn Reson Med. 2005;53(6):1432–1440.
9. Hui ES, Du F, Huang S, Shen Q, Duong TQ. Spatiotemporal dynamics of diffusional kurtosis, mean diffusivity and perfusion changes in experimental stroke. Brain Res. 2012;1451:100–109.
10. McKinnon ET, Fridriksson J, Glenn GR, et al. Structural plasticity of the ventral stream and aphasia recovery. Ann Neurol. 2017;82(1):147–151.
11. Fridriksson J, Rorden C, Elm J, Sen S, George MS, Bonilha L. Transcranial direct current stimulation vs sham stimulation to treat aphasia after stroke: a randomized clinical trial. JAMA Neurol. 2018;75(12):1470–1476.
12. Kertesz A. Western Aphasia Battery-Revised. The Psychological Corporation; 2007.
13. Roach A, Schwartz MF, Martin N, Grewal RS, Brecher A. The Philadelphia Naming Test: scoring and rationale. Clin. Aphasiol. 1996;24:121–133.
14. Veraart J, Novikov DS, Christiaens D, Ades-aron B, Sijbers J, Fieremans E. Denoising of diffusion MRI using random matrix theory. NeuroImage. 2016;142:394–406.
15. Kellner E, Dhital B, Kiselev VG, Reisert M. Gibbs-ringing artifact removal based on local subvoxel-shifts. Magn Reson Med. 2016;76(5):1574–1581.
16. Fridriksson J, Yourganov G, Bonilha L, Basilakos A, Den Ouden D-B, Rorden C. Revealing the dual streams of speech processing. Proc Natl Acad Sci USA. 2016;113 (52):15108–15113.
17. Hickok G, Poeppel D. The cortical organization of speech processing. Nat Rev Neurosci. 2007;8(5):393–402.
18. Liu M, Vermuri, BC. A robust and efficient doubly regularized metric learning approach [Internet]. In: Fitzgibbon, A, Lazebnik, S, Perona, P, Sato, Y, Schmid, C, eds. Computer Vision – ECCV 2012. Lecture Notes in Computer Science. Vol 7575. Berlin, Heidelberg: Springer; 2012. https://doi.org/10.1007/978-3-642-33765-9_46
19. Sokolov A, Carlin DE, Paull EO, Baertsch R, Stuart JM. Pathway-based genomics prediction using generalized elastic net. PLOS Comput Biol. 2016;12 (3):1004790.
20. Umesh Rudrapatna S, Wieloch T, Beirup K, et al. Can diffusion kurtosis imaging improve the sensitivity and specificity of detecting microstructural alterations in brain tissue chronically after experimental stroke? Comparisons with diffusion tensor imaging and histology. NeuroImage. 2014;97:363–373.
21. Zatorre RJ, Fields RD, Johansen-Berg H. Plasticity in gray and white: neuroimaging changes in brain structure during learning. Nat Neurosci. 2012;15(4):528–536.
22. Fridriksson J, den Ouden D-B, Hillis AE, et al. Anatomy of aphasia revisited. Brain. 2018;141(3):848–862.
23. Graves WW, Grabowski TJ, Mehta S, Gupta P. Left posterior superior temporal gyrus participates specifically in accessing lexical phonology. J Cogn Neurosci. 2008;20 (9):1698–1710.
24. Okada K, Hickok G. Identification of lexical-phonological networks in the superior temporal sulcus using functional magnetic resonance imaging. NeuroReport. 2006;17 (12):1293–1296.
25. Saffran EM. Aphasia and the relationship of language and brain. Semin Neurol. 2000;20(4):409–418.
26. Hickok G, Okada K, Serences JT. Area Spt in the human planum temporale supports sensory-motor integration for speech processing. J Neurophysiol. 2009;101(5):2725–2732.
27. Davey J, Thompson HE, Hallam G, et al. Exploring the role of the posterior middle temporal gyrus in semantic cognition: integration of anterior temporal lobe with executive processes. NeuroImage. 2016;137:165–177.
28. Whitney C, Kirk M, O'Sullivan J, Lambon Ralph MA, Jefferies E. The neural organization of semantic control: TMS evidence for a distributed network in left inferior frontal and posterior middle temporal gyrus. Cereb Cortex. 2010;21(5):1066–1075.
29. Lazar RM, Minzer B, Antoniello D, Festa JR, Krakauer JW, Marshall RS. Improvement in aphasia scores after stroke is well predicted by initial severity. Stroke. 2010;41 (7):1485–1488.
30. Marchi NA, Ptak R, Di Pietro M, Schnider A, Guggisberg AG. Principles of proportional recovery after stroke generalize to neglect and aphasia. Eur J Neurol. 2017;24 (8):1084–1087.
31. Skipper-Kallal LM, Lacey EH, Xing S, Turkeltaub PE. Right hemisphere remapping of naming functions depends on lesion size and location in poststroke aphasia. Neural Plast. 2017;1–17.

32. Stockert A, Wawrzyniak M, Klingbeil J, et al. Dynamics of language reorganization after left temporo-parietal and frontal stroke. Brain. 2020;23:844–861.
33. Musso M, Weiller C, Kiebel S, Müller SP, Bülau P, Rijntjes M. Training-induced brain plasticity in aphasia. Brain. 1999;122(Pt 9):1781–1790.
34. Saur D, Lange R, Baumgaertner A, et al. Dynamics of language reorganization after stroke. Brain. 2006;129(Pt 6):1371–1384.
35. Rijntjes M. Mechanisms of recovery in stroke patients with hemiparesis or aphasia: new insights, old questions and the meaning of therapies. Curr Opin Neurol. 2006;19 (1):76–83.

Supporting Information

Additional supporting information may be found online in the Supporting Information section at the end of the article.

Figure S1. Thirty regions of interests defined by the Johns Hopkins University. Regions of interests are associated with the ventral and dorsal stream of language and its right hemisphere homologous structures.
Figure S2. Relationship between change in mean kurtosis from baseline to 1 week after treatment and lesion volume in the posterior superior temporal gyrus (pSTG) for responders (colored in green; participants who produced more correct responses after treatment compared to baseline) and non-responders (colored in red; participants who produced less or equal number of correct responses after treatment compared to baseline).
Figure S3. Relationship between mean kurtosis at baseline and lesion volume in the precentral gyrus (PoCG) for responders (colored in green; participants who produced more correct responses after treatment compared to baseline) and non-responders (colored in red; participants who produced less or equal number of correct responses after treatment compared to baseline).
Figure S4. Relationship between mean kurtosis at baseline and lesion volume in the supramarginal gyrus (SMG) for responders (colored in green; participants who produced more correct responses after treatment compared to baseline) and non-responders (colored in red; participants who produced less or equal number of correct responses after treatment compared to baseline).
Figure S5. Relationship between mean kurtosis at baseline and lesion volume in the angular gyrus (AG) for responders (colored in green; participants who produced more correct responses after treatment compared to baseline) and non-responders (colored in red; participants who produced less or equal number of correct responses after treatment compared to baseline).
Figure S6. Relationship between change in mean kurtosis from baseline to 1 week after treatment and lesion volume in the middle temporal gyrus (MTG) for responders (colored in green; participants who produced less semantic errors after treatment compared to baseline) and non-responders (colored in red; participants who produced more or equal number of semantic errors after treatment compared to baseline).

